Heat exchange modeling between the air flow and the metro ventilation shaft lining in the conditions of St. Petersburg, Russia

Evgeny Kozin[1] and *Yuri* Kozhukhov[2,3*]

[1] SUE «St. Petersburg Metropoliten», Moskovsky Ave. 28, 190013, Saint-Petersburg, Russian Federation
[2] ITMO University, Kronverksky Ave., 49, lit. A, 197101, Saint-Petersburg, Russian Federation
[3] Peter the Great St.Petersburg Polytechnic University, Politechnicheskaya str. 29, 195251, Saint-Petersburg, Russian Federation

Abstract. Icing of the injection layer in underground tunnels and ventilation shafts leads to wear, destruction of supporting structures and flooding. In St. Petersburg the air temperature in winter can drop to -25 ° C, what can lead to these phenomena in the subway facilities. The article presents the modeling results of a viscous three-dimensional air flow, heat and mass transfer of a metro ventilation shaft in the Ansys CFX program. A numerical model of the ventilation shaft and the surrounding soil consisting of five layers has been developed: air; foam glass concrete; prefabricated cast-iron tubing lining; injection layer; soil massif. The parameters of the computational grid and the boundary conditions of the problem are specified. Two models of the ventilation shaft with an axial length of 1 m and 10 m were built. Temperature plots are constructed for three tasks, where the injection layer consists of water, wet clay soil and average between water and wet clay soil. The choice of overall thermal and technical characteristics of the thermal insulation material during the reconstruction of the existing ventilation shafts in three different sealing space conditions is confirmed. **Keywords:** ventilation shaft, lining, air flow, icing, forced convection, thermal convection, heat transfer, CFD.

1 Introduction

The main task of metro ventilation shafts is continuous air exchange at stations and running lines to ensure the quality and optimal microclimate of the air environment. The complex of ventilation facilities consists of a ground ventilation kiosk (ventilatory), a vertical shaft and ventilation tunnels and chambers.

Ventilation of the main tracks is organized in such a way that in winter the shafts supply cold air to the stages so that it warms up when moving along them before entering the station. The air temperature in winter can drop to -25 ° C and below, which leads to freezing of both the lining and soils along its contour. When the soils and water freeze in the sealing space, the lining experiences significant additional loads. This leads to

* Corresponding author: kozhukhov_yv@mail.ru

significant wear of vent structures, deformations and damage to tubing, up to their destruction and release of water and ground masses, i.e. to emergency situations.

Similar problems are found in many underground transport structures in the world, for example, in railway tunnels located in the cold regions of China [1]. The article [1] presents four technologies to prevent tunnel icing: installation of a drainage channel with frost protection for dewatering groundwater; installation of centralized drainage of deep occurrence; drainage channel to prevent freezing; thermal insulation layer. Heat from geological formations can also be used, for example, a scheme with a heat pump is proposed in [2] for heating the lining of the *Zilashan* tunnel.

At the studied object a thermal insulation jacket made of foam-glass concrete constructed inside a cast-iron tubing lining was used to prevent freezing of the sealing space. The design and strength of the material combines the solution of two main tasks at once: strengthening the existing lining with simultaneous provision of its thermal insulation.

To confirm the thermal insulation properties and thickness of the selected material, numerical modeling was performed - cast iron tubing has a complex geometric shape. Numerical modeling of heat transfer and aerodynamics will be successfully applied in construction and mining [3-7]. In [7], two types of thermal insulation materials are considered: polyurethane with a thickness of 100 mm and polyurethane with a thickness of 100 mm on the surface of the reinforced concrete jacket of the *Wufengshan* tunnel. Modeling of air flow at a speed of 0.5 m /s, a temperature of -20 ° C for 90 days and a constant rock temperature of +5 ° C showed that the freezing distance of rock to 0 ° C is 0.46 m from the sealing space, and the temperature in the sealing space is -9.5 ° C. When using thermal insulation materials, the temperature at this point will be slightly more than +3.1 ° C for the first material and +3.6 ° C for the second material. Full-scale tests with exposure to negative temperatures from -5 ° C to -15 ° C for 60 days showed a temperature in the sealing space of about -2 and +2 ° C in two segments without thermal insulation. In the segment with thermal insulation, the temperature in the sealing space was +4.8 ° C. These results indicate the effectiveness of numerical modeling for the analysis of heat transfer and selection of thermal insulation materials.

Based on the above, the actual purpose of this study is to simulate heat exchange during forced convection in the ventilation shaft with a selected layer of thermal insulation (foam concrete jackets).

2 Object and materials

For numerical modeling, the following layers shown in the diagram Fig. 1 have been developed. Layers consist of the following materials: 1 - air; 2 - foam glass concrete; 3 - prefabricated cast-iron tubing lining [8]; 4 - injection layer; 5 - soil massif. The axial length of each layer is 1 m.

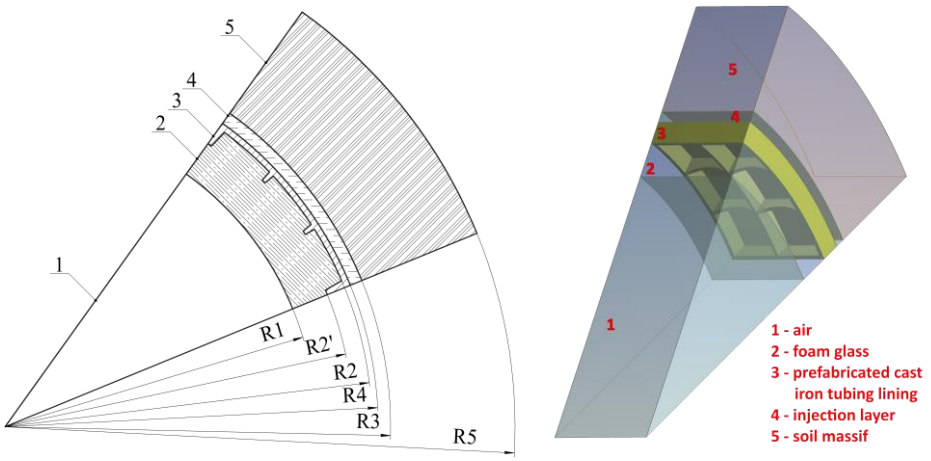

Fig. 1. Ventilation shaft segment a) layer diagram and b) CAD model; 1 - air; 2 - foam glass concrete; 3 - prefabricated cast iron tubing lining; 4 - injection layer; 5 - soil massif); control radii: R1= 2.480 m; R2'= 2.800 m; R2=2.965 m; R3= 3.000 m; R4=3.100 m; R5=4.100 m.

Table 1 shows the thermal characteristics of the materials used for the layers.

Table 1. Materials thermal characteristics.

Layer №		Material	Thermal conductivity coefficient, λ, W/(m·°C)	Heat capacity, C, J/(t·°C)
1		Air	0.0223	1006 000
2		Foam glass concrete	0.15	840 000
3		Cast iron	54.00	447 000
4	4.1	Water	0.57	4 190 000
	4.2	Wet clay soil	1.57	1 760 000
	4.3	Average values	1.00	3 000 000
5		Ground massif	1.75	880 000

In the article [9] for the Novosibirsk metro, it was found that the influence of seasonal changes in atmospheric air temperature on the soil mass in contact with the upper overlap of the station is limited by the depth of the stations - 11 m.

3 Mathematical model

The following provisions are adopted to perform the simulation:

1. The constant temperature at the outer boundary of the soil at a distance of 1 m from the injection layer is accepted as: 8 ° C (281.15 K). For example, according to [10] for Moscow, the natural ground temperature at a depth of 10 m is t_{gr} = 8.3 °C during the cold season.
2. The total air pressure at the entrance to the mine is atmospheric, P* = 101325 Pa.
3. The heat exchange along the circumference of the mine lining is uniform, so the angular segment of the shaft is calculated.
4. Gravitational forces are not modeled, since forced air movement in the mine is considered.
5. Working environments are continuum.
6. The mode of air movement is established in time.

7. The walls of the flowing part of the shaft are considered to be hydraulically smooth.
8. The thermal contact between the calculated areas is considered ideal.
9. Reinforcing in the thermal insulation layer are not considered.

The Ansys CFX 18.0 calculation complex was used for modeling. The RANS equations were calculated using the low-Reynolds shear stress transport (SST) turbulence model [11], combining stability and accuracy of the boundary layer resolution of the two–parameter k-ω model [12] and the solution of the main flow of the k–ε model [13]. The working environment is a perfect gas. The normal flow rate was set at the input. The average static pressure was set at the output.

The computational grid consists of 2,986,494 elements developed in the Ansys Mesh v18.0 grid generator (Fig. 2, a): 1 – unstructured hexahedral grid, 2 – unstructured tetrahedral grid, 3 – unstructured tetrahedral grid, 4, 5 – structured hexahedral grid. On both sides, at the boundary of the air medium and the solid the elements of the grid are condensed to take into account the boundary layer with the value of the dimensionless wall coordinate no more than y+<2.

Boundary conditions were established for the computational model in Figure 2, b, executed in Ansys CFX-Pre v18.0:

The speed of the outside air in the mine is considered to be the maximum permissible – s = 6 m/s.

Total outside air temperature in the shaft, $T_{вх}$= -25°C (248.15 K).

The temperature of the soil massif at the outer boundary at a distance of 1 m from the injection layer is assumed to be equal to T_{const}=8°C (281.15 K).

Working material of the sealing space – water or wet loam soil.

The choice of the material of the sealing space is explained by the fact that during operation the cement composition of the primary and control injection (50...100 mm) is washed out and replaced by either water or soil.

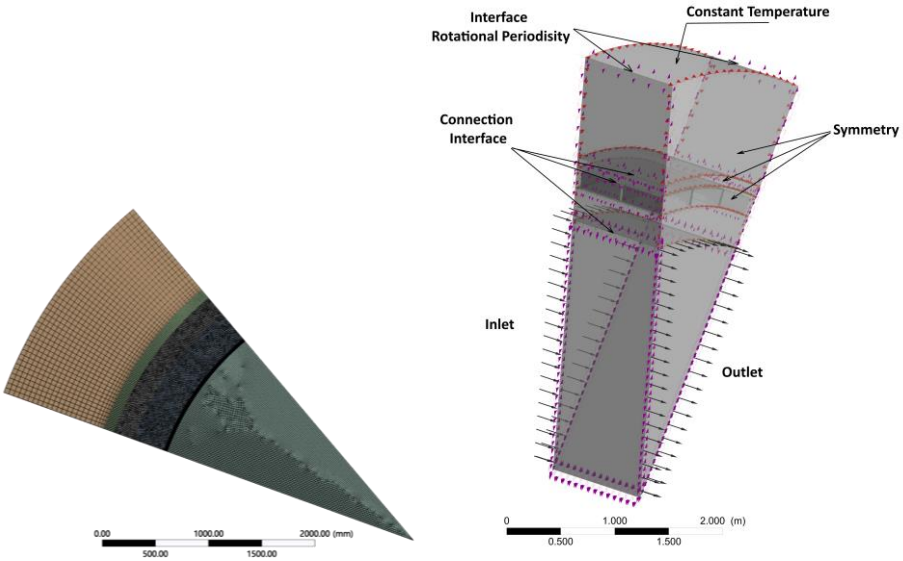

Fig. 2. The appearance of the calculated grids of layers and sectors of the calculated model; a) The scheme of the layers of the calculated grid of the ventilation shaft model; b) The CFD model of the segment with boundary conditions.

According to Table 1, three calculations were performed with three variants of the sealing space materials: water, wet loam soil, average value. The fourth calculation was

performed for a 10 m long shaft (the filling space is water) by combining ten calculation areas into a single unit with the calculation grid elements number of 29,864,940.

The converged solution of the numerical problem was obtained in about 200 iterations. The level of unbalance according to the conservation equations in all computational domains was no more than 10^{-8} starting from 150 iterations, which indicates the conservativeness of the solution. Additionally, a temperature monitoring point is installed in the sealing space. The calculation results illustrate the invariance of temperature from iteration to iteration starting from 70 iterations. Before the final calculation, a study was performed on the grid independence of the solution by comparing the original grid and the grid reduced by half, the same results were obtained.

4 Modeling results

Tables 2, 3, 4 summarize the results of modeling three tasks. In the first one, the worst situation is considered when the sealing space is filled with water. In the second task, the sealing space is a moist loam soil. In the third task some average values are shown.

Table 2. The value of average temperatures on the control surfaces T_{w5}=+8 °C (sealing space – water).

Location	Radius, m	Average temperature, °K	Average temperature, °C
On the inner wall of the foam-glass concrete shirt	R_1= 2.480	T_{w1}=248.58	-24.57
On the inner shell of cast iron tubing	R_2=2.965	T_{w2}=275.04	+1.89
On the outer shell of cast iron tubing	R_3= 3.000	T_{w3}=275.04	+1.89
On the outside of the sealing space	R_4=3.100	T_{w4}=276.66	+3.51
Temperature at the boundary of the soil massif (1 m from the lining)	R_5=4.100	T_{w5}=281.15	+8

Table 3. The value of average temperatures on the control surfaces at Tw5=+8 °C (sealing space – wet soil).

Location	Radius, m	Average temperature, °K	Average temperature, °C
On the inner wall of the foam-glass concrete shirt	R_1= 2.480	T_{w1}=248.60	-24.55
On the inner shell of cast iron tubing	R_2=2.965	T_{w2}=275.91	+2.76
On the outer shell of cast iron tubing	R_3= 3.000	T_{w3}=275.91	+2.76
On the outside of the sealing space	R_4=3.100	T_{w4}=276.52	+3.37
Temperature at the boundary of the soil massif (1 m from the lining)	R_5=4.100	T_{w5}=281.15	+8

Table 4. The value of the average temperatures on the control surfaces at Tw5=+8 °C (sealing space – average values).

Location	Radius, m	Average temperature, °K	Average temperature, °C
On the inner wall of the foam-glass concrete shirt	R_1= 2.480	T_{w1}=248.59	-24.56
On the inner shell of cast iron tubing	R_2=2.965	T_{w2}=275.62	+2.47
On the outer shell of cast iron tubing	R_3= 3.000	T_{w3}=275.62	+2.47
On the outside of the sealing space	R_4=3.100	T_{w4}=276.56	+3.41
Temperature at the boundary of the soil massif (1 m from the lining)	R_5=4.100	T_{w5}=281.15	+8

According to the simulation results, a positive temperature is provided for all variants in the sealing space. The minimum temperature is +1.89 °C, the maximum temperature is +2.76 °C.

Figure 3 shows the temperature epures of the ventilation shaft in the radial direction at a distance of 0.75 m for calculations No. 1, 2, 3 (the length of the calculated area is 1 m) and 9.75 m for calculation No. 4 (the length of the calculated area is 10 m).

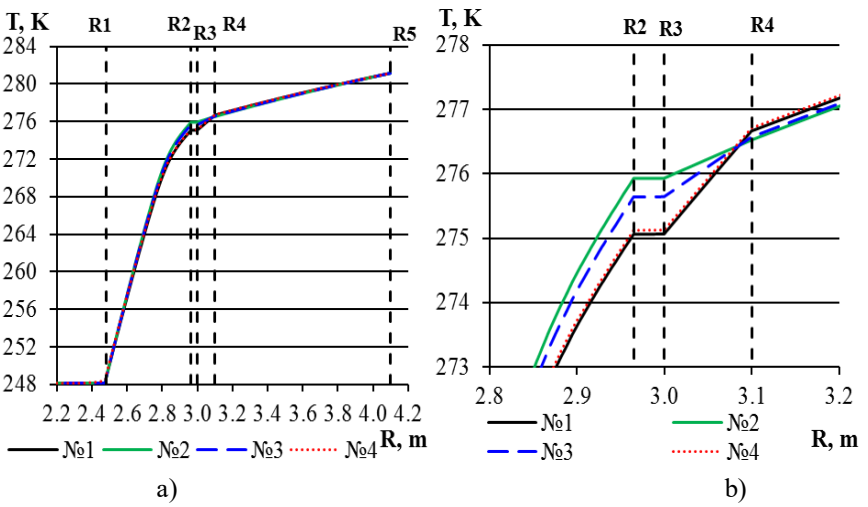

Fig. 3. Temperature epure of the ventilation shaft in the radial direction: a) in the range of radii 2.2-4.2 m, b) in the range of radii 2.2-3.2 m.

The epure shows the linear nature of the temperature change over 70% of the insulation thickness regardless of the material of the sealing space. The final temperature depends on the material of the sealing space, the temperature difference for all the considered options does not exceed 0.87 ° C.

The prefabricated cast-iron tubing lining has internal stiffening ribs. Figure 4 a show the isosurfaces of the temperature distribution in the radial plane at a distance of 9.5 m where the secant plane is located exactly along the central edge of stiffness and Figure 4 b show the secant plane is located between the central and lateral stiffening ribs. It is shown that the presence of cast-iron ribs has a positive effect on the heat transfer from the ground to the thermal insulation jacket. Periodic zones of temperature increase due to the presence of stiffening ribs are clearly visible in Figure 5.

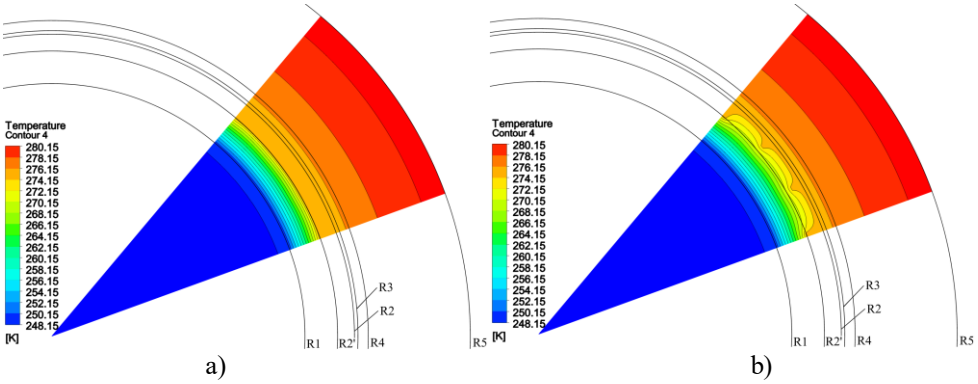

Fig. 4. Contours of temperature isosurfaces in the radial plane at a distance of a) 9.5 m and b) 9.75 m.

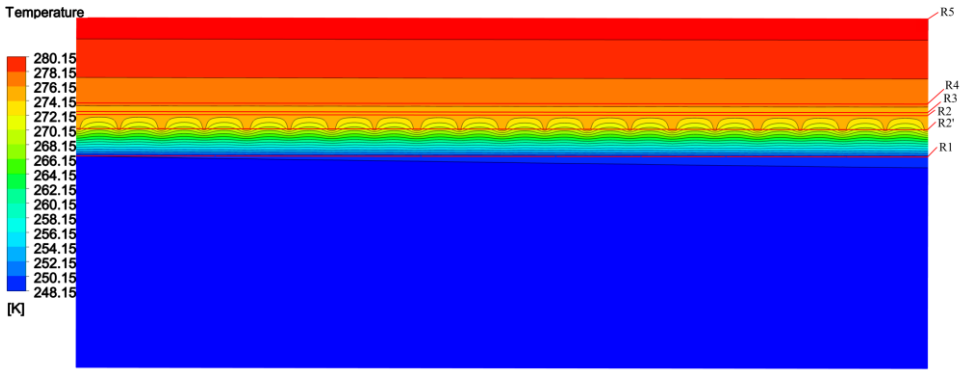

Fig. 5. Contours of isosurfaces temperature in the axial plane

Temperature epures at different radii of the ventilation shaft in the axial direction for 10 meters along the length of the shaft Z are shown in Figure 6. A slight change in temperature along the length of the ventilation shaft is visible.

The performed modeling demonstrates the absence of freezing in the sealing space with the selected type and thickness of the thermal insulation material.

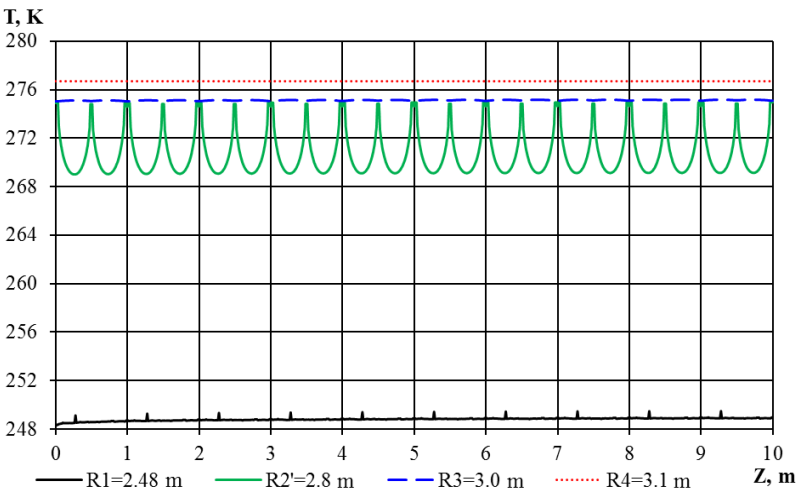

Fig. 6. Temperature epure of the ventilation shaft in the axial direction.

5 Conclusion

As a result of the study, modeling of one-meter and ten-meter segments of the metro ventilation shaft was carried out. Modeling of a one–meter segment was carried out for three conditions: the first – watering of the filling space and the working material is water, in the second condition - the working material is a wet loam soil and the third – a mixed medium of water and wet loam soil. According to the simulation results, there are no negative temperatures for all three conditions and, accordingly, there is no freezing of the shaft. The use of numerical modeling can help to choose the dimensions and necessary parameters of the foam glass concrete thermal insulation jacket.

References

1. Y. Luo, J. Chen, J. Traffic Transp. Eng. **6.3**, 297–309 (2019) Doi:10.1016/j.jtte.2018.09.007
2. X. Zhou et al, Tunn. Undergr. Sp. Technol **111**, 103843 (2021) Doi: 10.1016/j.tust.2021.103843
3. E.V. Kolesov, B.P. Kazakov, M.A. Semin, J. Min. Sci. **57.5**, 852–862 (2021) Doi: 10.1134/S106273912105015X
4. M.A. Semin, L.Y. Levin, Min. informational Anal. Bull. **6**, 151–167 (2020) Doi: 10.25018/0236-1493-2020-6-0-151-167
5. I.A. Gaas, S.A. Starcev, N.S. Har'kov, D.S. Shuravina, Stroitel'stvo unikal'nyh zdanij i sooruzhenij **1(16)**, 23-35 (2014) Doi: 10.18720/CUBS.16.2
6. A.M. Krasyuk, I.V. Lugin, A.Y. P'yankova, J Min Sci **51**, 138–143 (2015) https://doi.org/10.1134/S1062739115010184
7. G. Cui et al, Case Stud. Therm. Eng **28**, 101652 (2021) Doi: 10.1016/j.csite.2021.101652
8. *GOST R 57054—2016. Tyubingi chugunnye. Komplekty tyubingovyh kolec*
9. A.M. Krasyuk, I.V. Lugin, A.Y. P'yankova, J Min Sci **48**, 465–473 (2012) https://doi.org/10.1134/S1062739148030094
10. I.V. Lugin, E.L. Alferova, Gornyj informacionno-analiticheskij byulleten' **2**, 305–314 (2017) https://cyberleninka.ru/article/n/issledovanie-teplovogo-potoka-v-gruntovyy-massiv-iz-dvuhputnogo-tonnelya-metropolitena-melkogo-zalozheniya/viewer
11. F.R. Menter, AIAA-Journal **32(8)**, 1598 - 1605 (1994) DOI:10.2514/3.12149
12. D.C. Wilcox, AIAA J. (1988) DOI:10.2514/3.10042
13. B.E. Launder, B.I. Sharma, Letters in Heat and Mass Transfer **1(2)**, 131-138 (1974) DOI:10.1016/0094-4548(74)90150-7